Two linkers are better than one: Enhancing CO_2 capture and separation with porous covalent triazine-based frameworks from mixed nitrile linkers.

Subarna Dey,[a] Asamanjoy Bhunia,[a] Hergen Breitzke,[b] Pedro B. Groszewicz,[b] Gerd Buntkowsky[b] and Christoph Janiak[a,*]

[a] Institut für Anorganische Chemie und Strukturchemie, Heinrich-Heine Universität Düsseldorf, 40204 Düsseldorf, Germany.

[b] Eduard-Zintl-Institut, Technische Universität Darmstadt, Alarich-Weiss-Str. 8, 64287 Darmstadt

* Corresponding author: E-mail: janiak@uni-duesseldorf.de; Fax: + 49-211-81-12287; Tel: +49-211-81-12286.

Further emails: subarna.dey@hhu.de, asamanjoy.bhunia@gmail.com, breitzke@chemie.tu-darmstadt.de, groszewicz@chemie.tu-darmstadt.de, Gerd.Buntkowsky@chemie.tu-darmstadt.de

Table of contents

1. Experimental Section

Materials and methods

All chemicals were purchased from commercial suppliers (Sigma-Aldrich, Acros Organics, and Alfa Aesar chemical company) and used without further purification, unless stated otherwise. Tetrakis(4-cyanophenyl)ethylene was synthesized according to the reported procedures.[1]

Infrared (IR) spectra were obtained on a Bruker FT-IR Tensor 37 Spectrometer in the 4000-550 cm^{-1} region with 2 cm^{-1} resolution as KBr disks. **Solution ^{1}H and ^{13}C spectra** were recorded on a Avance DRX-500 instruments. **Elemental (CNH) analyses** were carried out with a PerkinElmer 2400 series 2 elemental analyzer. **Powder X-ray diffraction (PXRD)** data was collected on a Bruker D2 Phaser diffractometer using a flat sample holder (also a flat silicon, low background sample holder) and Cu $K\alpha_1/\alpha_2$ radiation with λ = 1.5418 Å at 30 kV covering 2theta angles 5-80° over a time of 2 h, that is. 0.01°/sec. Diffractograms were obtained on flat layer sample holders where at low angle the beam spot is strongly broadened so that only a fraction of the reflected radiation reaches the detector which leads to low relative intensities measured at $2\theta < 7°$. For hygroscopic or air-sensitive samples, the sample holder can be sealed with a dome. **Scanning electron microscopy (SEM)** images were obtained using an ESEM Quanta 400 FEG SEM equipped with a secondary electron detector for **energy-dispersive X-ray spectroscopy** or on a a Jeol JSM-6510LV QSEM Advanced electron microscope using a LAB-6 cathode at 5-20 keV. This microscope is equipped with a Bruker Xflash 410 silicon drift detector and the Bruker ESPRIT software for EDX analysis. **Thermogravimetric analyses (TGA)** were carried out at a ramp rate of 5 °C/min in a N_2 flow with a Netzsch Thermo-Microbalance Apparatus TG 209 F3 Tarsus.

X-ray photoelectron spectroscopy (XPS) analysis was performed on an ESCALAB Fisons/VG Scientific ESCALAB 200XPS Spectrometer. The spectra were obtained at a temperature of 70-80 °C and a vacuum of $1x10^{-9}$ mbar with pass energy of 50 eV and Al-Kα radiation ($h\nu$ = 1486.6 eV) operated at 200 W and 12 kV with total acquisition time of 8 min. The binding energy region from 200-600 eV was scanned for determining the C/N ratio.

Gas sorption isotherms were measured using a Micromeritics ASAP 2020 automatic gas sorption analyzer equipped with oil-free vacuum pumps (ultimate vacuum $<10^{-8}$ mbar) and valves, which guaranteed contamination free measurements. The sample was connected to the preparation port of the sorption analyzer and degassed under vacuum until the outgassing rate, i.e., the rate of pressure rise in the temporarily closed manifold with the connected sample tube, was less than 2 μTorr/min at the specified temperature 200 °C. After weighing, the sample tube was then transferred to the analysis port of the sorption analyzer. All used gases (H_2, He, N_2, CO_2, CH_4) were of ultra high purity (UHP, grade 5.0, 99.999%) and the STP volumes are given according to the NIST standards (293.15 K, 101.325 kPa). Helium gas was used for the determination of the cold and warm free space of the sample tubes. H_2 and N_2 sorption isotherms were measured at 77 K (liquid nitrogen bath), whereas CO_2 and CH_4 sorption isotherms were measured at 293±1 K (passive thermostating) and 273.15 K (ice/deionized water bath). The heat of adsorption values and the DFT pore size distributions ('N_2 DFT slit pore' model) were calculated out using the ASAP 2020 v3.05 software.

A **coulometric Karl-Fischer titration** for the determination of the water content was carried out with a Karl-Fischer titration apparatus AQUA 40.00 with headspace module. The solid CTF sample was heated to 170 °C in the head space module and the liberated water transferred to the measurement cell.

Water sorption isotherms at 20 °C were obtained volumetrically from a Quantachrome Autosorb iQ MP instrument equipped with an all-gas option. Prior to the sorption experiments, the compounds were degassed (130 °C, 2h) under dynamic vacuum.

^{1}H /^{19}F/^{13}C CP MAS solid state NMR measurements were carried out at room temperature on a Bruker AVANCE II^{+} spectrometer at 400 MHz for ^{1}H resonance frequency, employing a Bruker 3.2 mm H/F/X/Y MAS probe. ^{1}H/^{19}F/^{13}C CP MAS spectra were recorded utilizing ramped CP-MAS sequences at spinning rates of 8 kHz. Contact times were set to 1.5 ms and tppm decoupling with a 20° phase jump was applied during data acquisition.
^{1}H /^{19}F/^{13}C CP MAS spectra were recorded under various decoupling conditions i.e. applying ^{1}H, ^{19}F decoupling only for ^{1}H/^{13}C and ^{19}F/^{13}CP, respectively, and applying ^{1}H/^{19}F decoupling simultaneously during data acquisition.
High resolution ^{1}H and ^{19}F spectra were recorded on a Bruker AVANCE III Spectrometer at 600 MHz ^{1}H resonance frequency employing a Bruker 1.3 mm H/X MAS Probe at 50 kHz spinning rate at room temperature.
^{1}H/^{13}C LG-HETCOR spectrum was recorded at 12 kHz spinning speed and 1.5 ms contact time. LG-decoupling field strength was set to 75 kHz, ^{1}H tppm decoupling with a 20° phase jump was applied during data acquisition. Indirect dimension referencing was done by setting the correlation peak to the chemical shift of the aromatic peak of the ^{1}H high speed MAS spectrum recorded at 600 MHz.
^{13}C and ^{1}H solid state NMR spectra were referenced to tetramethylsilane, ^{19}F spectra were referenced with respect to $CFCl_3$.

2. Synthesis of CTFs (MM1-MM4)

- reaction temperature 400 °C

MM1: A mixture of tetrakis(4-cyanophenyl)ethylene (100 mg, 0.23 mmol), terephthalonitrile (60 mg, 0.46 mmol) and $ZnCl_2$ (940 mg, 6.19 mmol) were placed into a Pyrex ampoule under inert conditions. The ampoule was evacuated, sealed and heated to 400 °C for 48 h followed by cooling to room temperature. The black product was collected and stirred with water for 72 h. Then the product was isolated by filtration and again stirred with 100 mL of 2 mol/L HCl for 24 h. The resulting black powder was further washed with water (3 × 50 mL), THF (3 × 30 mL), acetone (3 × 30 mL) and dried in vacuum. Yield: 130 mg, 81 %.

MM2: A mixture of tetrakis(4-cyanophenyl)ethylene (100 mg, 0.23 mmol), tetrafluoroterephthalonitrile (92 mg, 0.46 mmol) and $ZnCl_2$ (940 mg, 6.91 mmol) were placed into a Pyrex ampoule under inert conditions. The ampoule was evacuated, sealed and heated to 400 °C for 48 h followed by cooling to room temperature. The black product was collected and stirred with water for 72 h. Then the product was isolated by filtration and again stirred with 100 mL of 2 mol/L HCl for 24 h. The resulting black powder was further washed with water (3 × 50 mL), THF (3 × 30 mL), acetone (3 × 30 mL) and dried in vacuum. Yield: 137 mg, 71 %.

MM3: A mixture of tetrakis(4-cyanophenyl)ethylene (75 mg, 0.17 mmol), 4,4′-biphenyldicarbonitrile (71 mg, 0.35 mmol) and $ZnCl_2$ (713 mg, 5.34 mmol) were placed into a Pyrex ampoule under inert conditions. The ampoule was evacuated, sealed and heated to 400 °C for 48 h followed by cooling to room temperature. The black product was collected and stirred with water for 72 h. Then the product was isolated by filtration and again stirred with 100 mL of 2 mol/L HCl for 24 h. The resulting black powder was further washed with water (3 × 50 mL), THF (3 × 30 mL), acetone (3 × 30 mL) and dried in vacuum. Yield: 127 mg, 87 %.

MM4: A mixture of tetrakis(4-cyanophenyl)ethylene (86 mg, 0.2 mmol), 1,3,5-benzenetricarbonitrile (40 mg, 0.26 mmol) and $ZnCl_2$ (627 mg, 4.6 mmol) were placed into a Pyrex ampoule under inert conditions. The ampoule was evacuated, sealed and heated to 400 °C for 48 h followed by cooling to room temperature. The black product was collected and stirred with water for 72 h. Then the product was isolated by filtration and again stirred with 100 mL of 2 mol/L HCl for 24 h. The resulting black powder was further washed with water (3 × 50 mL), THF (3 × 30 mL), acetone (3 × 30 mL) and dried in vacuum. Yield: 105 mg, 83 %.

- other reaction temperatures:

MM2-300: A mixture of tetrakis(4-cyanophenyl)ethylene (**M**, 100 mg, 0.23 mmol), tetrafluoroterephthalonitrile (**M2**, 92 mg, 0.46 mmol) and $ZnCl_2$ (940 mg, 6.91 mmol) were placed into a Pyrex ampoule under inert conditions. The ampoule was evacuated, sealed and heated to 300 °C for 48 h followed by cooling to room temperature. The black product was collected and stirred with water for 72 h. Then the product was isolated by filtration and again stirred with 100 mL of 2 mol/L HCl for 24 h. The resulting black powder was further washed with water (3 × 50 mL), THF (3 × 30 mL), acetone (3 × 30 mL) and dried in vacuum.

MM2-600: A mixture of tetrakis(4-cyanophenyl)ethylene (**M**, 100 mg, 0.23 mmol), tetrafluoroterephthalonitrile (**M2**, 92 mg, 0.46 mmol) and $ZnCl_2$ (940 mg, 6.91 mmol) were placed into a quartz ampoule under inert conditions. The ampoule was evacuated, sealed and heated to 600 °C for 48 h followed by cooling to room temperature. The black product was collected and stirred with water for 72 h. Then the product was isolated by filtration and again stirred with 100 mL of 2 mol/L HCl for 24 h. The resulting black powder was further washed with water (3 × 50 mL), THF (3 × 30 mL), acetone (3 × 30 mL) and dried in vacuum.

MM4-600: A mixture of tetrakis(4-cyanophenyl)ethylene (**M**, 86 mg, 0.2 mmol), 1,3,5-benzenetricarbonitrile (**M4**, 40 mg, 0.26 mmol) and $ZnCl_2$ (627 mg, 4.6 mmol) were placed into a quartz ampoule under inert conditions. The ampoule was evacuated, sealed and heated to 600 °C for 48 h followed by cooling to room temperature. The black product was collected and stirred with water for 72 h. Then the product was isolated by filtration and again stirred with 100 mL of 2 mol/L HCl for 24 h. The resulting black powder was further washed with water (3 × 50 mL), THF (3 × 30 mL), acetone (3 × 30 mL) and dried in vacuum.

3. Elemental analysis of MM1-MM4

Table S1a Elemental analysis of MM1-MM4 (combustion analysis

Material [a]	Calculated (%) [b]					Found (%)				
	C	H	N	C/H	C/N	C	H	N	C/H	C/N
MM1	80.22	3.51	16.27	1.9	5.7	79.09	2.52	5.77	2.6	16.0
MM2	66.35	1.94	13.45	2.9	5.7	65.43	4.02	10.73	1.4	7.1
synth.300°C	66.35	1.94	13.45	2.9	5.7	67.12	3.25	12.83	1.7	6.1
MM3	82.84	3.84	13.33	1.8	7.3	79.15	2.87	3.19	2.4	28.9
MM4	79.23	3.17	17.6	2.10	5.24	74.99	3.46	9.79	1.8	8.9

[a] Synthesis at 400 °C unless mentioned otherwise.

[b] Calculated based on the following formulae according to the used stoichiometric ratios (without considering the adsorption of moisture (see below):

MM1 :

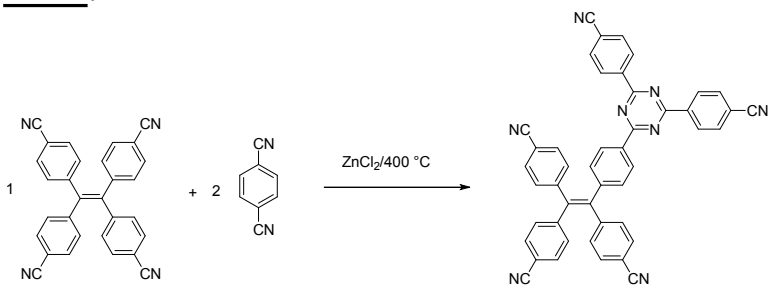

$C_{30}H_{16}N_4$ $C_8H_4N_2$ $C_{46}H_{24}N_8$

Molecular Weight: 688.74

MM2 :

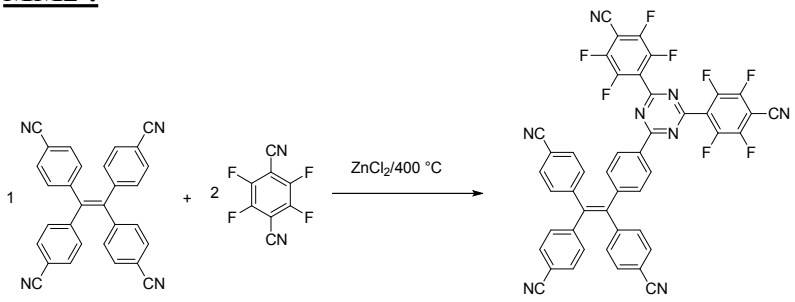

$C_{30}H_{16}N_4$ $C_8F_4N_2$ $C_{46}H_{16}F_8N_8$, *Molecular Weight: 832.66*

MM3 :

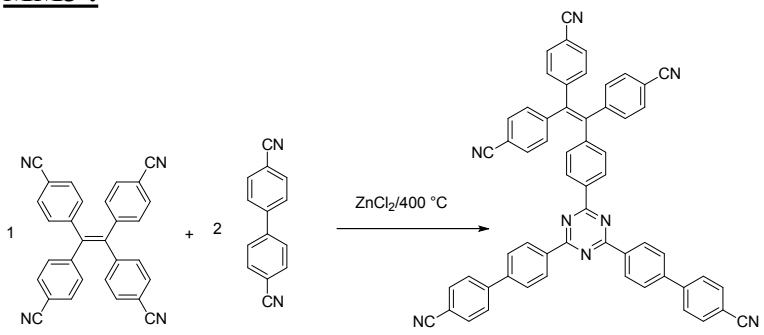

$C_{30}H_{16}N_4$ $C_{14}H_8N_2$ $C_{58}H_{32}N_8$, *Molecular Weight: 840.93*

MM4 :

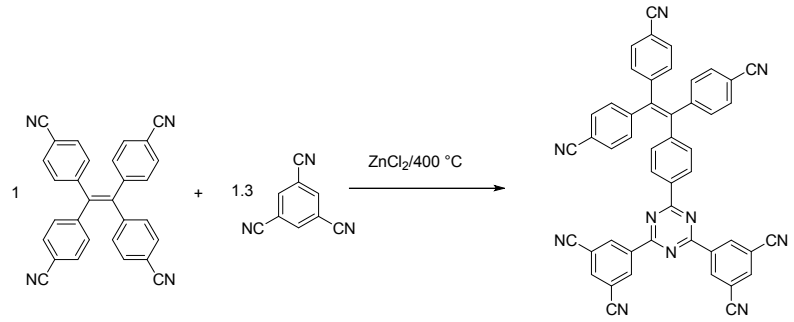

$C_{30}H_{16}N_4$ *$C_9H_3N_3$* *~$C_{42}H_{20}N_8$, Molecular Weight: 636*

The elemental analysis of MM1-MM4 give a much lower nitrogen content and concomitantly a much higher than calculated C/N ratio. This indicates that most of the nitrogen is lost due to decomposition (Scheme S1).

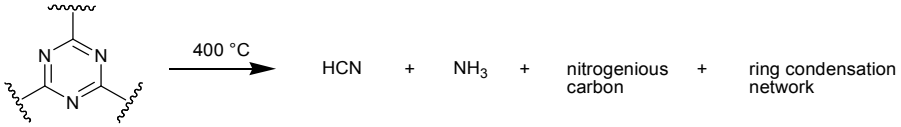

Scheme S1 General schematic representation for the decomposition of a triazine ring.

The mismatch in N-content (calculated and found) is a combination of triazine ring decompositions together with residual $ZnCl_2$. We note that the powder diffractograms for MM1, MM3 and MM4 show a distinct peak at $2\theta = 17.2°$ which is assigned to the (111) plane from $ZnCl_2$. It is these MM'-CTFs which also have the lowest N content.

However irregular distributions of the M and M1-4 building units in the resulting CTFs cannot be responsible as even the separate reaction of M and M' only with itself, which would give a mixture of M-CTF and M'-CTF, would still have to give the same theoretical C, H, N values for this mixture than for the ideal MM'-CTF. Also, unreacted –CN functional sites cannot explain the deviation as the polymerization reaction retains the full monomer formula content, that is, even the mixture of monomers will have the same calculated C, H, N values as the ideal MM'-CTF product.

Table S1b Elemental analysis of MM1-MM4 from energy-dispersive X-ray spectroscopy (EDX) and X-ray photoelectron spectroscopy (XPS)

	EDX		XPS		CHN
Element@MM1	atom% [a]	C/N [d]	atom% (%286 eV) [c]	C/N [d]	molar C/N found [d]
C	91.2	13.6	93.9 (11)	15.4	16.0
N	6.7		6.1		
Zn	0.7		n.d.		
Cl	0.4		n.d.		
Element@MM2(400 °C)					
C	86.1	6.7	87.5 (30)	7.0	7.1
N	12.8		12.5		
F	0.6		(1) [e]		
Zn	0.2		n.d.		
Cl	0.2		n.d.		
Element@MM2(300 °C) [b]					
C	77.4	7.0			6.1
N	11.1				
F	11.5	(F:N=1.0)			
Element@MM3					
C	94.6	19.3	95.0 (14)	19.0	28.9
N	4.9		5.0		
Zn	0.3		n.d.		
Cl	0.2		n.d.		
Element@MM4					
C	90.3	10.1	90.9 (20)	10.0	8.9
N	8.9		9.1		
Zn	0.5		n.d.		
Cl	0.4		n.d.		

[a] Based on the Kα lines. Note that quantification of atom% values for non-neighboring element is prone to large errors because of different cross-sections for the K-shell electron ionization together with different matrix effects for absorption of the emitted X-ray photons.

[b] Average from two samples with two EDX sampled regions each. The molar F:N ratio of 1.0 is the required ratio from the above formulae according to the used stoichiometric ratios.

[c] C and N content set to 100%. The value in parenthesis is the share (in %) of the tail contribution to the C 1s peak.

The C 1s peak (with a maximum at ~284 eV) can be de-convoluted into two or even three contributions and has a pronounced tail towards 286 eV. The peak-tail at ~286 eV can be assigned to C-N bound carbon atoms. The trend of a larger percentage of the 286 eV peak coincides with a larger amount of nitrogen found in the material. n.d. = not determined.

- see graphics below (on next three pages for C1s regions.

[d] Carbon and nitrogen quantification by EDX and XPS are in excellent agreement concerning atom% amount and molar C/N ratio. The trend in the molar C/N ratio also agrees with the molar ratio determined by combustion analysis.

[e] Only a very small F 1s peak, barely about the noise level, could be detected with low accuracy (see following graphic).

X-ray spectroscopy (XPS) of sample MM2(400 °C)

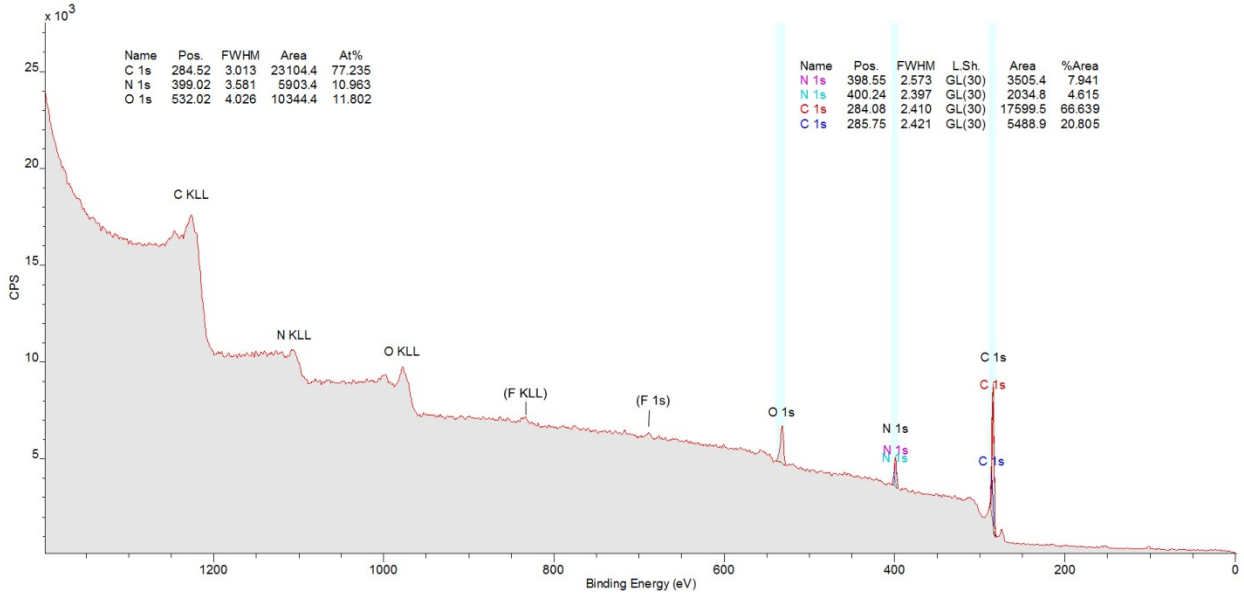

X-ray spectroscopy (XPS) of MM' samples (400 °C)

C 1s region for MM1. Contribution at 285.7 eV (11.2%), 284.6 eV (26.7%), 283.6 (62.1%):

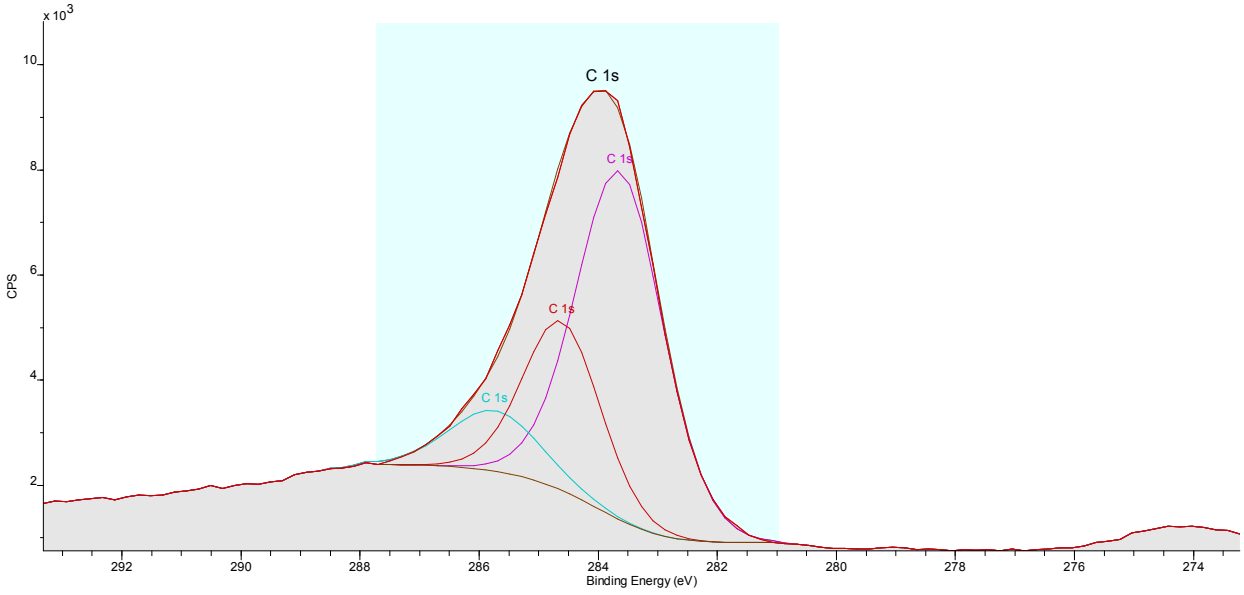

C 1s region for MM2. Contribution at 285.0 eV (30.3%), 283.8 (69.7%):

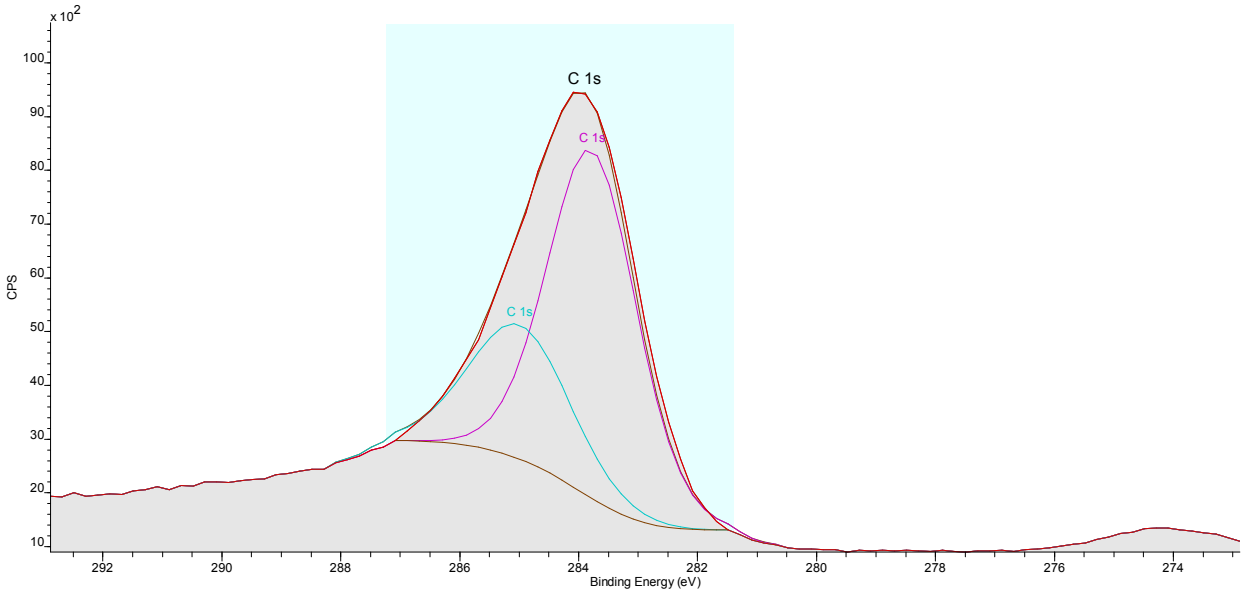

C 1s region for MM3. Contribution at 285.5 eV (13.9%), 284.0 (86.1%):

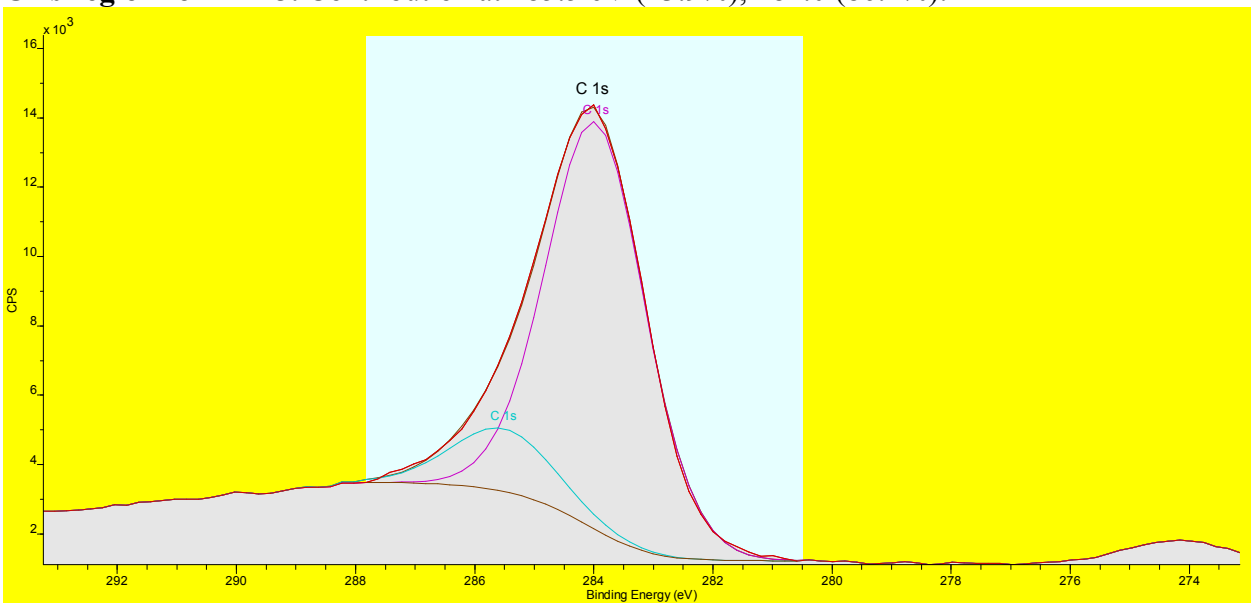

C 1s region for MM4. Contribution at 285.4 eV (20.4%), 283.8 (79.6%):

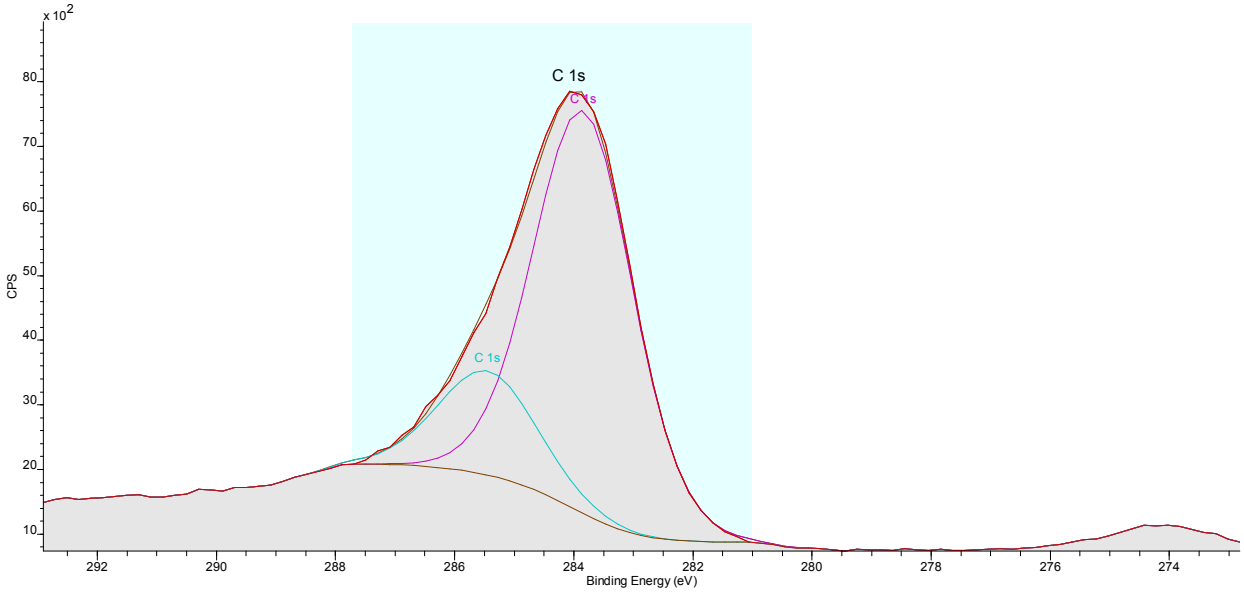

The presence of hydrated zinc and zinc hydroxide species would lead to chemisorption of CO_2 according to: [Zn]-OH + CO_2 --> [Zn]-OCO_2H

However, from the formed Zn-bicarbonate the CO_2 would not be released again at room temperature. So, in our CO_2 sorption isotherms we should then have seen a hysteresis which does not close towards p --> 0 mmHg. Most likely, the above uptake of CO_2 from ambient air by hydrated Zn species will have already occurred upon storage of the sample under air. Therefore, we are confident that the CO_2 uptake from gas sorption reflects the uptake by the porosity of the network and not by the Zn species.

4. Powder X-ray diffraction (PXRD) patterns of MM1-MM4

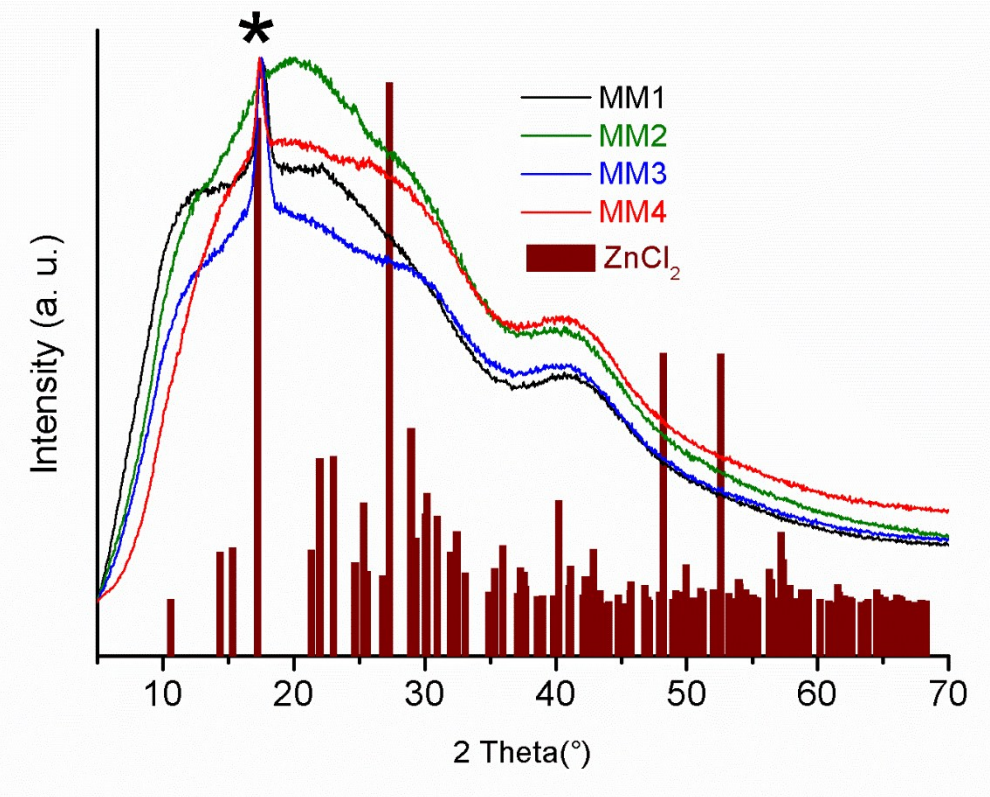

Fig. S1: Powder X-ray pattern of MM1-MM4 and its comparison with $ZnCl_2$. Single peak with * is from $ZnCl_2$ for the (111) plane at $2\theta = 17.2°$.[2]

5. Thermogravimetric analysis (TGA)

All materials (MM1-MM4) show definite weight loss before decomposition. Both weight loss and decomposition temperature are summarized in Table S2.

Table S2 Decomposition temperature for MM1-MM4.

Compound	Decomposition Temperature (°C)	Weight loss at decomposition temperature (%)	Weight loss until 100-150 °C temperature range (%)
MM1	440	7.4	3.2
MM2	460	19.02	9.5-10.4
MM3	385	10.96	3.1-3.2
MM4	450	10.95	2.7-2.9

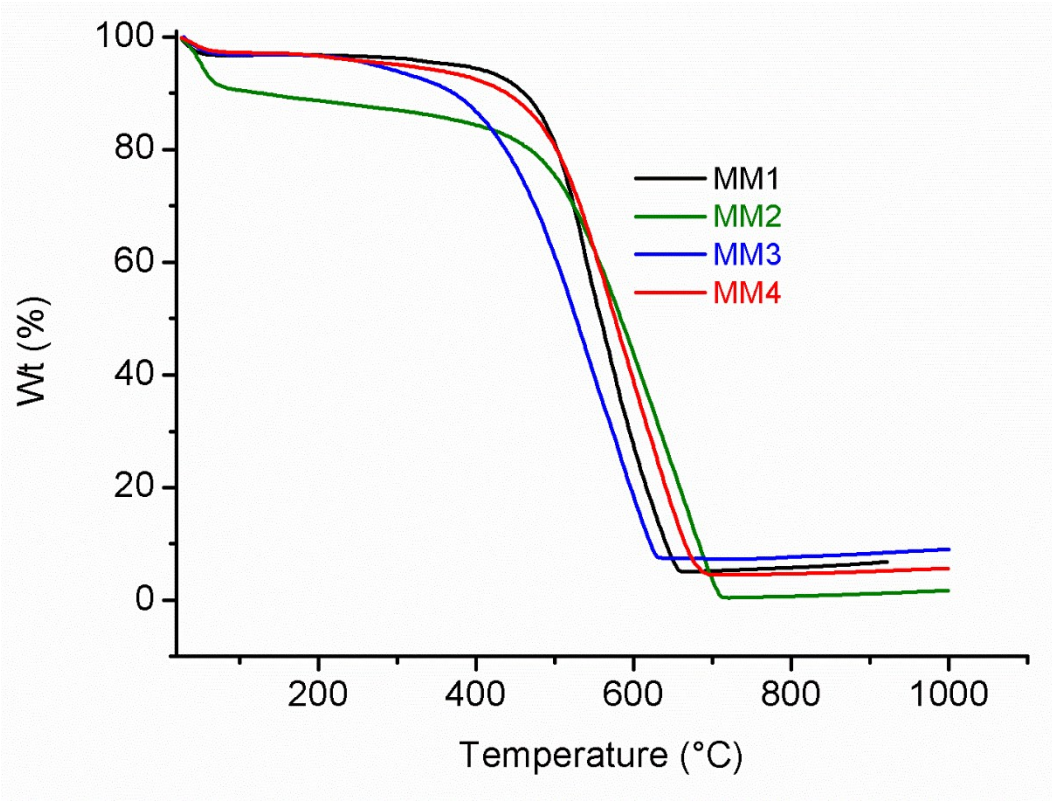

Fig. S2: TGA for MM1-MM4 in temperature range of 25 to 1000 °C at the heating rate of 5 °C / min.

6. Selectivity from initial slopes in the Henry region

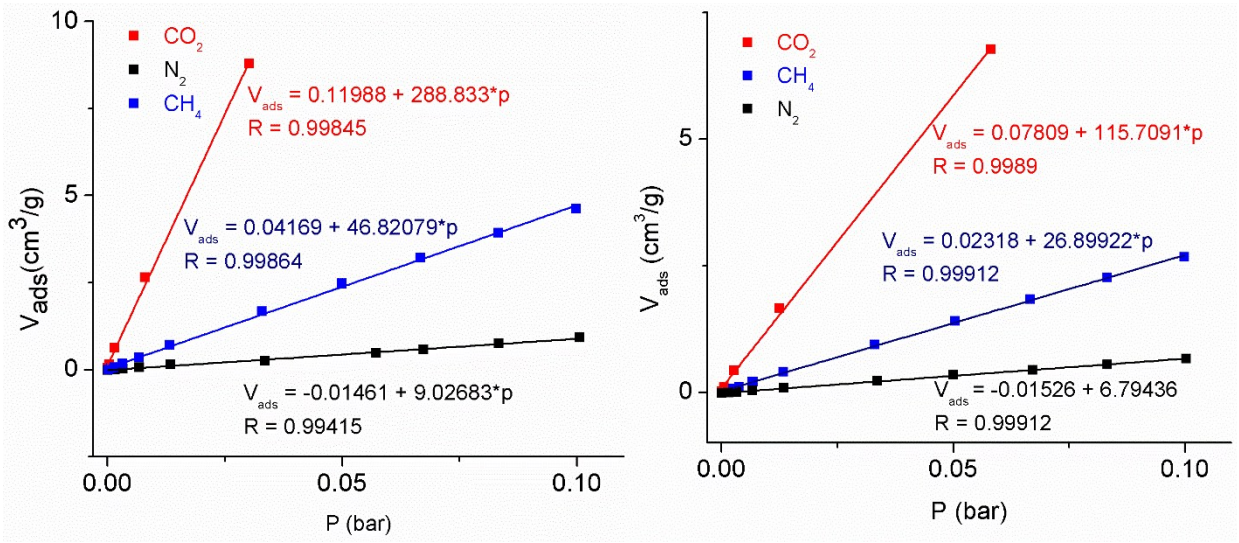

Fig. S3: The initial slopes in the Henry region of the adsorption isotherms for MM1 at 273 K (left) and 293 K (right).

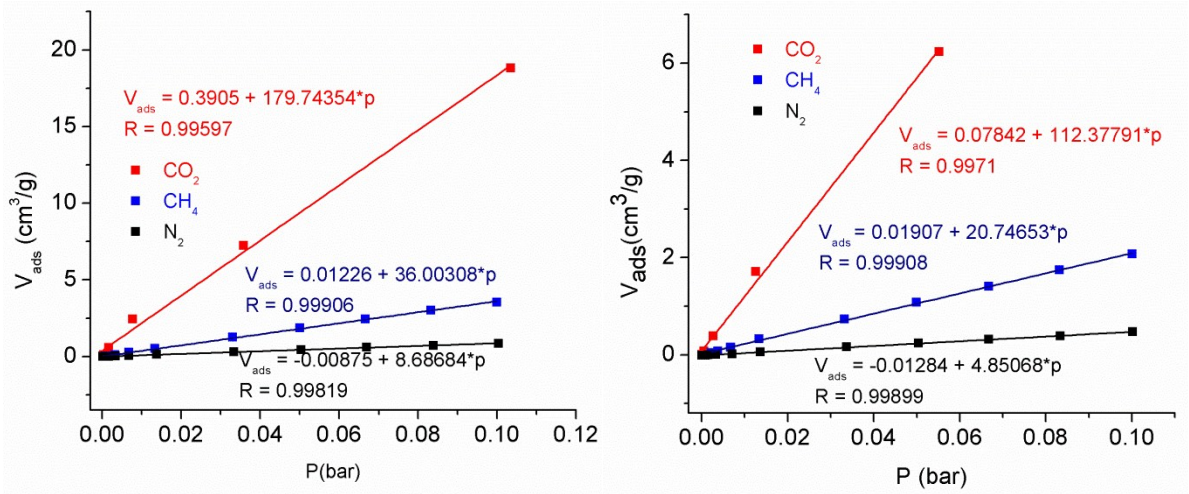

Fig. S4: The initial slopes in the Henry region of the adsorption isotherms for MM2 at 273 K (left) and 293 K (right).

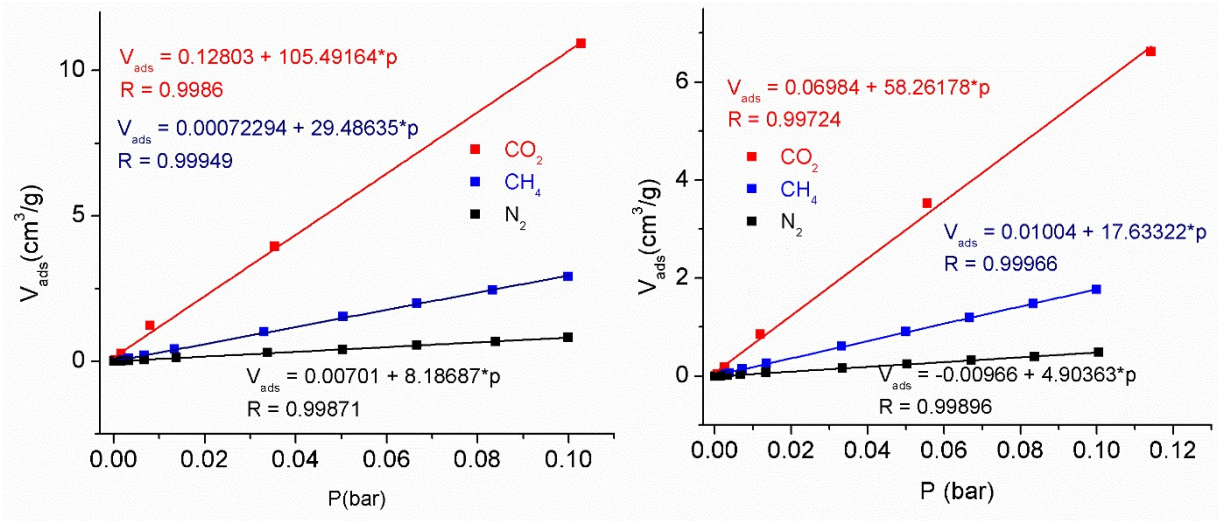

Fig. S5: The initial slopes in the Henry region of the adsorption isotherms for MM3 at 273 K (left) and 293 K (right).

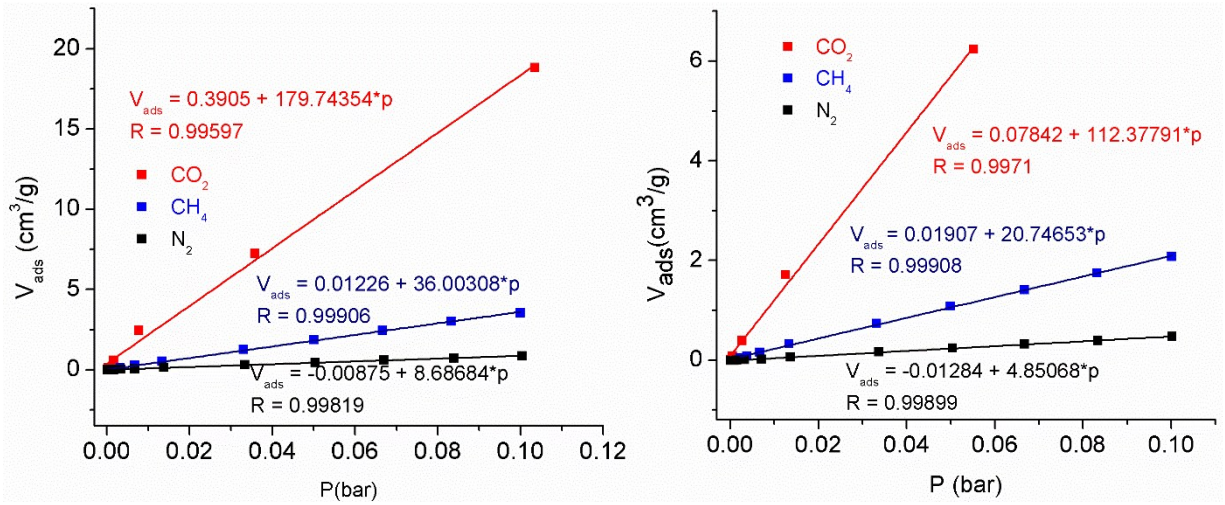

Fig. S6: The initial slopes in the Henry region of the adsorption isotherms for MM4 at 273 K (left) and 293 K (right).

7. Ideal Adsorbed Solution Theory (IAST) selectivity studies

IAST selectivities were calculated from the gas adsorption data using a single or dual-site Langmuir model to fit the adsorption isotherms. For CO_2 adsorption isotherm up to 1 bar, we assumed the double-layer adsorption. Therefore, the low pressure (up to 1 bar) adsorption isotherms of CO_2 measured at 273 K was fitted with the dual-site Langmuir (DSL) model. The equation is:

$$q = q_A + q_B = q_{sat,A}\frac{b_A p}{1 + b_A p} + q_{sat,B}\frac{b_B p}{1 + b_B p}$$

Where, q is molar uptake of adsorbate (mmol/g), q_{sat} is saturation uptake (mmol/g), b is the parameter in single component Langmuir isotherm (bar^{-1}), p is the pressure of bulk gas, the subscription of A and B refers to different two sites.

On the other hand, due to the mono-layer adsorption of CH_4 and N_2 adsorption, the single-site Langmuir models were used:

$$q = q_{sat}\frac{bp}{1 + bp}$$

The IAST selectivity S_{ads} can be calculated from the following equation:

$$S_{ads} = \frac{q1/q2}{p1/p2}$$

A CO_2:N_2 ratio of 15:85 was used for calculating the gas mixture selectivities, which is typically the flue gas composition.

Table S3 Langmuir fitting parameters of CO_2, CH_4, and N_2 adsorption isotherms of MM1, MM2, MM3 and MM4 at 273 K and 1 bar (synthesized at 400 °C).

MM1@273K	$q_{sat,A}$ (mmol/g)	b_A (bar^{-1})	$q_{sat,B}$ (mmol/g)	b_B (bar^{-1})	Adj. R^2
CO_2	0.79922	12.12842	9.64014	0.44951	0.99999
CH_4	3.33385	0.62106			0.9996
N_2	4.6281	0.0974			0.99997

MM2@273K	$q_{sat,A}$ (mmol/g)	b_A (bar^{-1})	$q_{sat,B}$ (mmol/g)	b_B (bar^{-1})	Adj. R^2
CO_2	1.21485	14.75997	9.04758	0.67154	0.99998
CH_4	3.542	0.693			0.99968
N_2	2.84484	0.18657			0.99997

MM3@273K	$q_{sat,A}$ (mmol/g)	b_A (bar^{-1})	$q_{sat,B}$ (mmol/g)	b_B (bar^{-1})	Adj. R^2
CO_2	0.4344	8.28541	10.16668	0.28643	1
CH_4	3.45169	0.37891			0.9999
N_2	2.88644	0.12548			0.9999

MM4@273K	$q_{sat,A}$ (mmol/g)	b_A (bar^{-1})	$q_{sat,B}$ (mmol/g)	b_B (bar^{-1})	Adj. R^2
CO_2	0.83529	11.16812	7.98059	0.50873	0.9999
CH_4	3.15435	0.51096			0.99985
N_2	2.74336	0.13795			0.99998

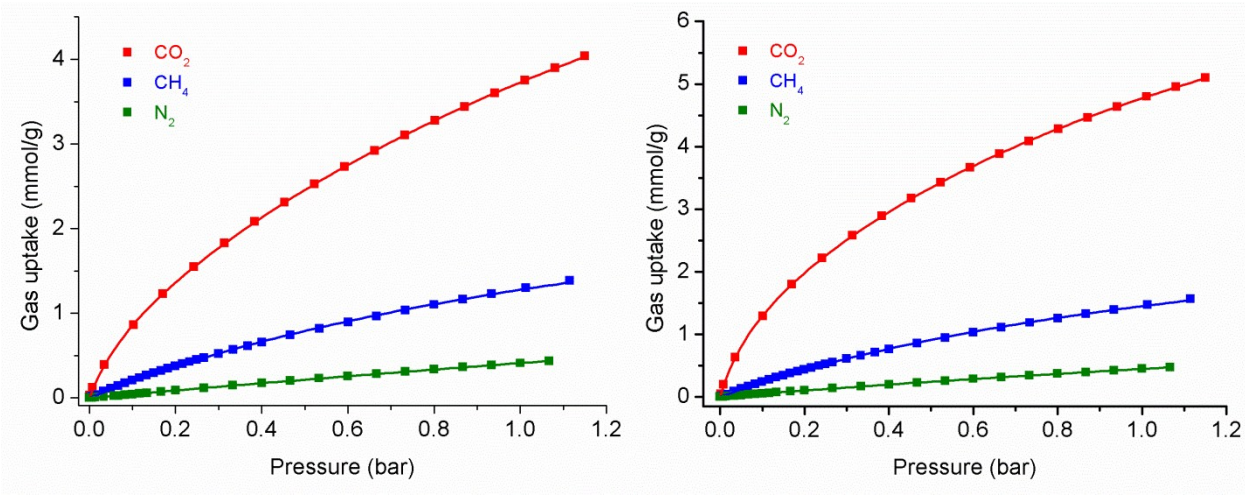

Fig. S7: DSL fitting for CO_2 adsorption and SSL fittings for CH_4 and N_2 adsorption at 273 K for MM1 (left) and MM2 (right).

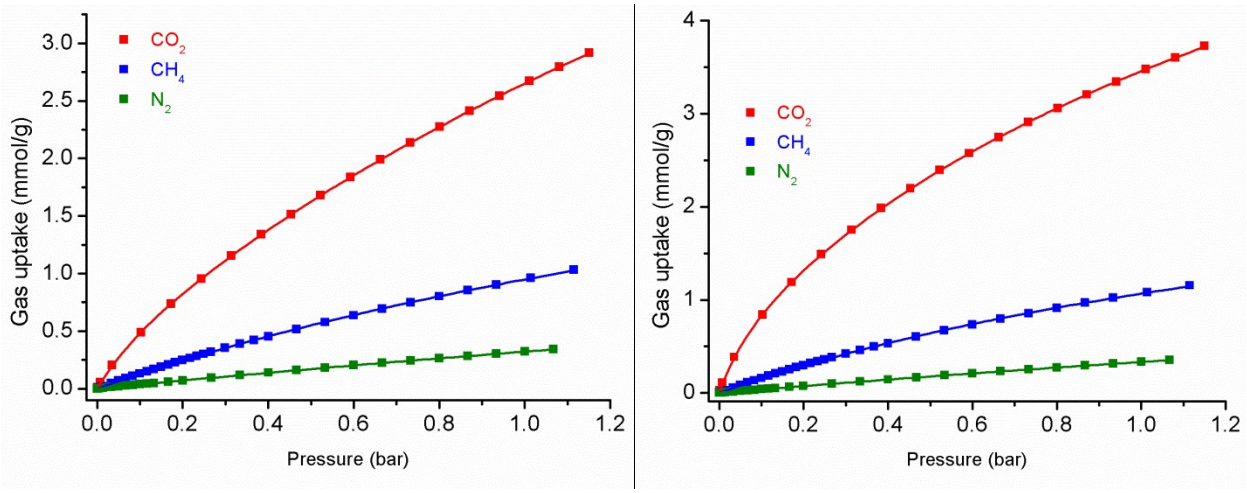

Fig. S8: DSL fitting for CO_2 adsorption and SSL fittings for CH_4 and N_2 adsorption at 273 K for MM3 (left) and MM4 (right).

8. Karl Fischer Titration

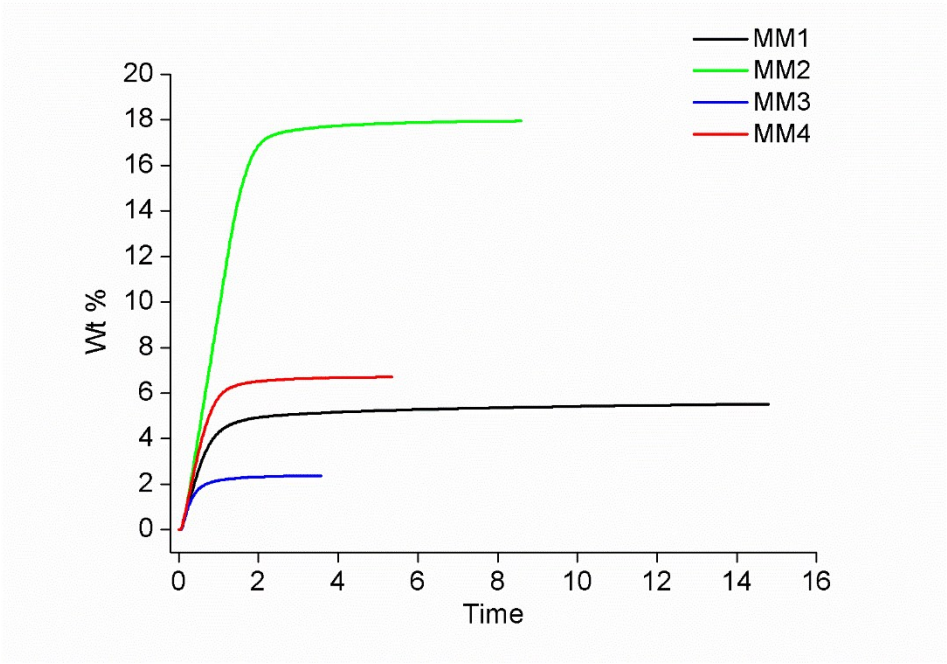

Fig. S9: Karl-Fisher Titration plot for MM1-MM4

Table S4 Amount of water absorbed on CTFs measured by Karl-Fisher Titration

CTFs [a]	Water loading (wt %)
MM1	5.1
MM2	17.5
MM3	1.9
MM4	6.3

[a] Sample had been stored under ambient air with about 50% air humidity.

9. Water adsorption isotherms

Table S5 Water uptake values for MM1- MM4 at 20 °C

CTFs	Uptake at $P/P_0 = 0.1$		Uptake at $P/P_0 = 0.5$		Uptake at $P/P_0 = 0.9$ [a]		V_{tot} [b]
	cm^3/g	g/g	cm^3/g	g/g	cm^3/g	g/g	cm^3/g
MM1	12	0.0096	140	0.11	622	0.498	1.11
MM2	44	0.035	377	0.3	548	0.439	0.67
MM3	7	0.0056	56	0.04	948	0.7596	1.52
MM4	17	0.0136	205	0.17	480	0.384	0.78

[a] The uptake near saturation pressure is not so much determined by the hydrophilicity but by the porosity and available pore volume V_{tot} due to capillary condensation

[b] Total pore volume at $P/P_0 = 0.95$ for pores ≤20 nm (repeated from Table 1 in paper).

10. Comparison to other CTFs

Table S6 Surface area, CO_2 adsorption properties and selectivity of triazine-based polymer.

Compound	BET (m^2/g)	CO_2 uptake (mmol/g) at 1 bar [a]		Q_{st}	CO_2/N_2 selectivity [b]		Ref.
		273 K	298 K or 293 K		Henry	IAST	
CTF-0-400-600	2011	4.22					3
CTF-1	746	2.47	1.41	27.5		20	4
CTF-1-600	1533	3.82	2.25	30.0		13	4
FCTF-1	662	4.67	3.21	35.0		31	4
FCTF-1-600	1535	5.53	3.41	32		19	4
CTF-P2	776	1.84				20.3	5
CTF-P3	571	2.22				22.5	5
CTF-P4	867	3.05				16.6	5
CTF-P5	960	2.94				24.1	5
CTF-P6	1152	3.32				16.1	5
CTF-P1M	4	0.92				31.2	5

CTF-P2M	464	1.87				21.0	5
CTF-P3M	523	2.21				15.8	5
CTF-P4M	542	1.83				22.4	5
CTF-P5M	542	2.03				20.1	5
CTF-P6M	947	4.12				14.2	5
MCTP-1	1452	4.61	2.70				6
MCTP-2	859	3.65	2.46				6
Polymer 2	--	--	1.56				7
Polymer 3	646	--	1.68				7
Polymer 4	1266	--	2.09				7
Polymer 2C	427	--	2.99				7
Polymer 3C	1173	--	3.08				7
Polymer 4C	1316	--	3.61				7
NOP-1	978	1.83	1.06	32.8			8
NOP-2	1055	2.37	1.40	34.1			8
NOP-3	1198	2.51	1.39	33.8	27.1	25.6	8
NOP-4	635	1.71	0.83	31.9			8
NOP-5	913	1.45	0.72	30.5			8
NOP-6	1130	1.31	0.49	29.2	33.7	38.7	8
MCTF-300	640	2.25	1.39	24.6			9
MCTF-400	1060	2.36	1.55	25.4			9
MCTF-500	1510	3.16	2.22	26.3			9
fl-CTF300	15	1.27	0.71	43.1	35	37	10
fl-CTF350	1235	4.28	2.29	32.7	27	23	10
fl-CTF400	2862	4.13	1.97	30.7	15	16	10
fl-CTF500	2322	3.26	1.65	31.7	13	12	10
fl-CTF600	2113	3.48	1.80	32.4	14	12	10
COP-1	168	--	1.33				11
COP-2	158		0.91				11
PCTF-1	2235	3.26	1.84	30	13	17 [b]	12

PCTF-2	784	1.85	0.992	26	9	13 [b]	12
PCTF-3	641	2.17	1.32	27	16	34 [b]	12
PCTF-4	1090	2.30	1.49	28	17	35 [b]	12
PCTF-5	1183	2.59	1.48	27	17	39 [b]	12
PCTF-6	79	--	--		--	--	12
PCTF-7	613	2.18	1.32	25	22	--	12
HPF-1	576	--	2.8	43		120	13
CTF-TPC	1668	4.24	2.47	32			14
CTF-FL	773	3.26	2.00	35			14
MM1	1800	3.68	2.17	32	32	130	This work
MM2	1360	4.70	2.88	36	23	97	This work
MM3	1884	2.62	1.51	43	13	77	This work
MM4	1407	3.40	2.05	30	21	98	This work

[a] Transformation into cm^3/g can be done by the given value in mmol/g with the molar gas volume at 1 bar of 22.711 L/mol (or mL/mmol = $cm^3/mmol$) (at 273 K), 24.375 L (at 293) and 24.791 L (at 298).

Alternatively, transformation from given cm^3/g into mmol/g:

at 273 K: value in (cm^3/g) : (22.711 $cm^3/mmol$) = value in (mmol/g)
(22.711 L is the molar volume at 1 bar and 273 K for an ideal gas).

at 293 K: value in (cm^3/g) : (24.375 $cm^3/mmol$) = value in (mmol/g)
(24.375 L is the molar volume at 1 bar and 293 K for an ideal gas).

Conversion to value in g/g = value in (mmol/g) x (0.044 g/mmol) from which the value wt% is obtained as $g(CO_2)/g(CO_2+adsorbent)$ x 100%.

[b] at 1 bar for an equimolar gas mixture.

11. Scanning electron micrograph of MM1-MM4

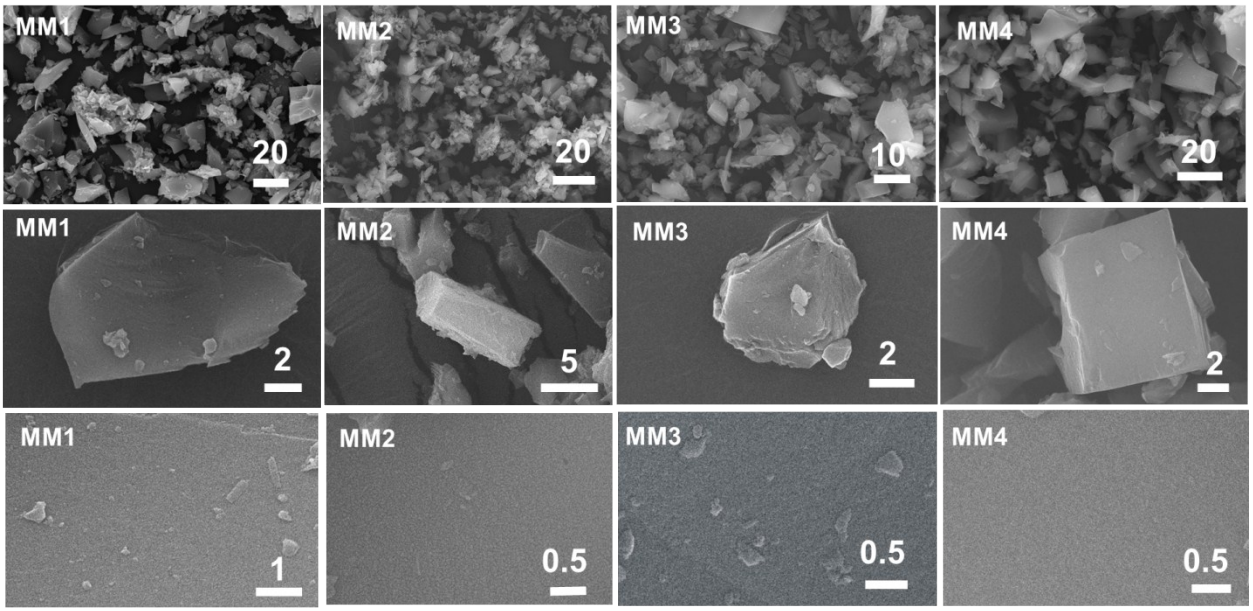

Fig. S10 Scanning electron micrographs of MM1 - MM4 (numbers above the scale bar are in μm). Enlarged version of Fig. 2 in paper.

12. Virial equation analysis of CO_2 adsorption data for calculation of the Q_{st} values

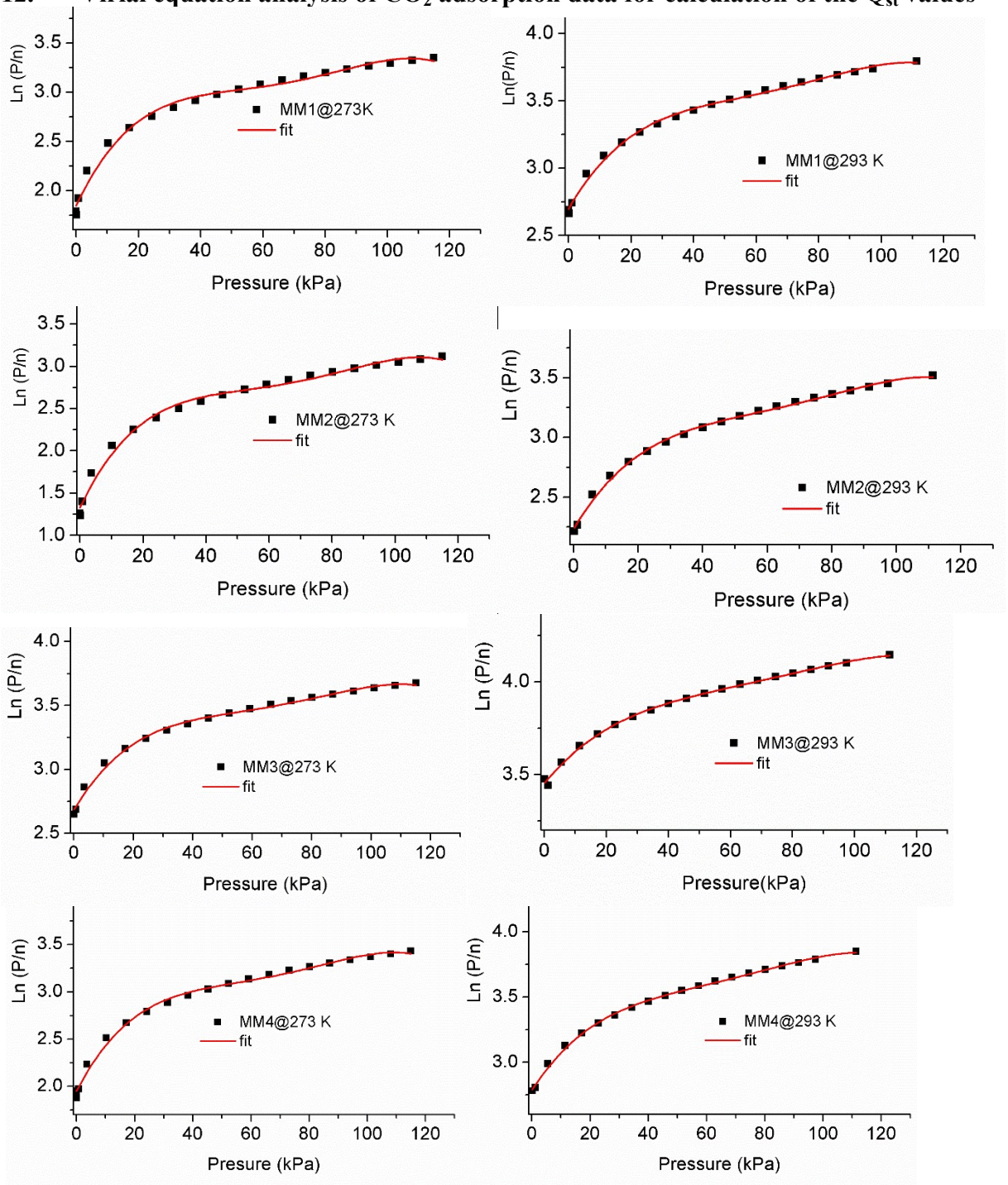

Fig. S11 Virial equation analysis of CO_2 adsorption data fitting.

From these fittings we have calculated the Q_{st} values for MM1-MM4 (see Fig. 8 in main manuscript).

13. Gas sorption of MM'-CTF materials synthesized at 300 °C and 600 °C (MM2-300, MM2-600 and MM4-600)

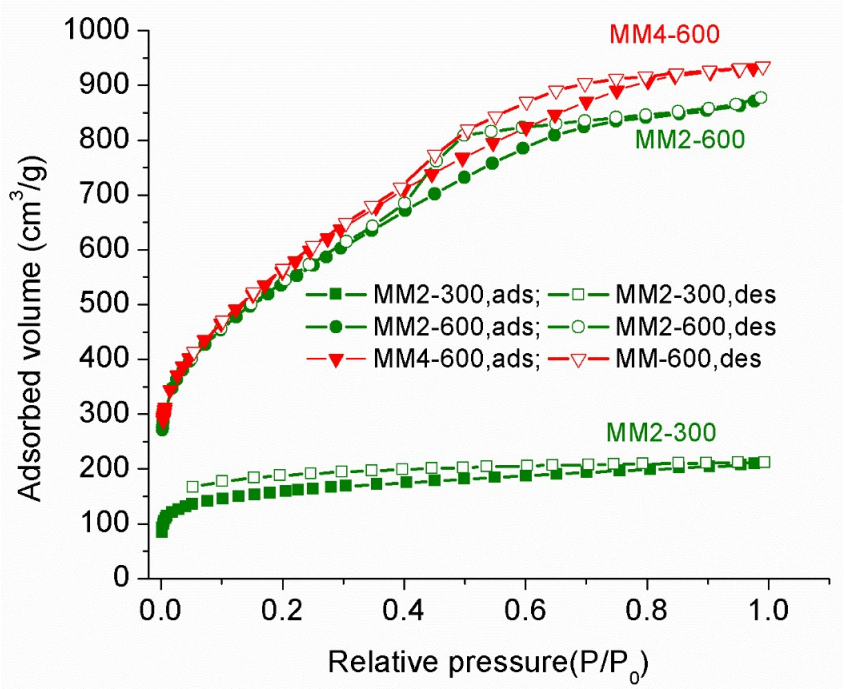

Fig. S12 Nitrogen adsorption-desorption isotherms (closed symbols for adsorption and open symbols for desorption) for MM2-300, MM2-600 and MM4-600 (-300 and -600 are the synthesis temperatures in °C).

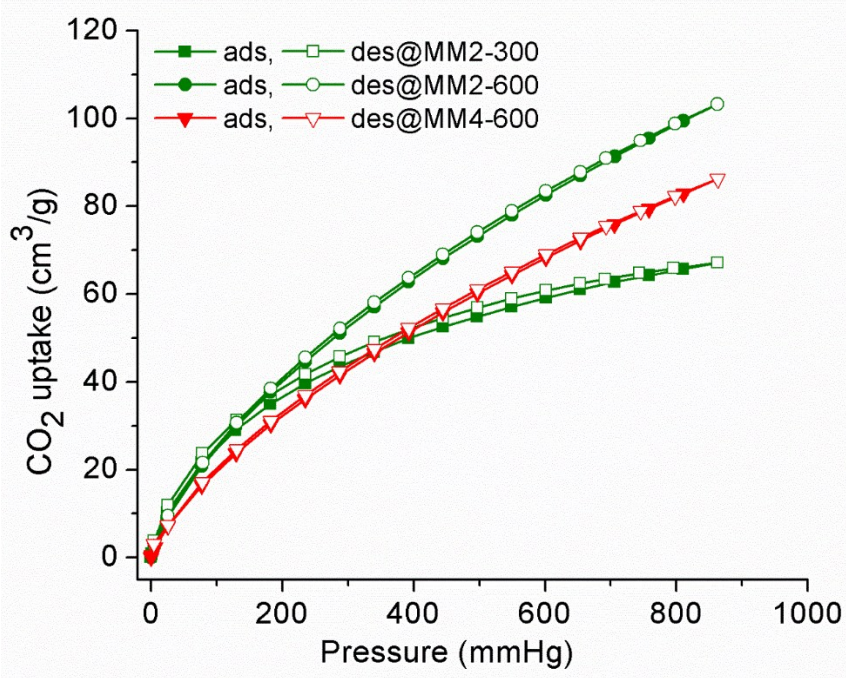

Fig. S13 CO_2 sorption isotherms at 273 K and 1 bar for MM2-300, MM2-600 and MM4-600 (-300 and -600 are the synthesis temperatures in °C).

14. Solid-state NMR spectroscopy

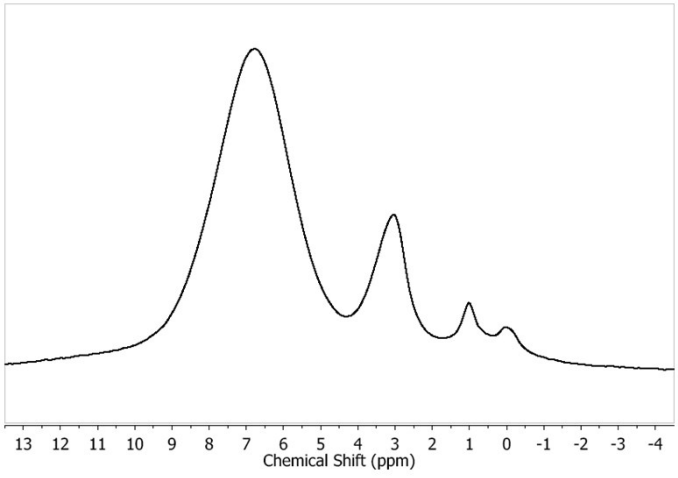

(a)

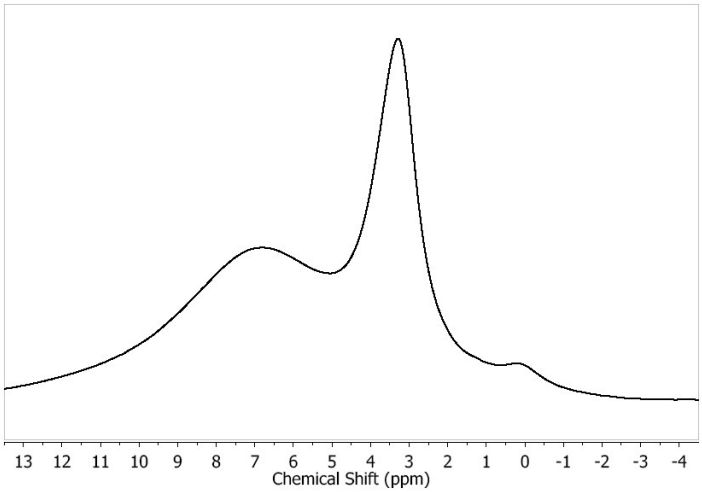

(b)

Fig. S14 Solid-state ^{1}H MAS spectrum of MM2(300) at a) 50 kHz b) 12 kHz. In the 50 kHz spectrum the intensity ratio of the signal at 7 ppm relative to the other small signals combined is 14:1.

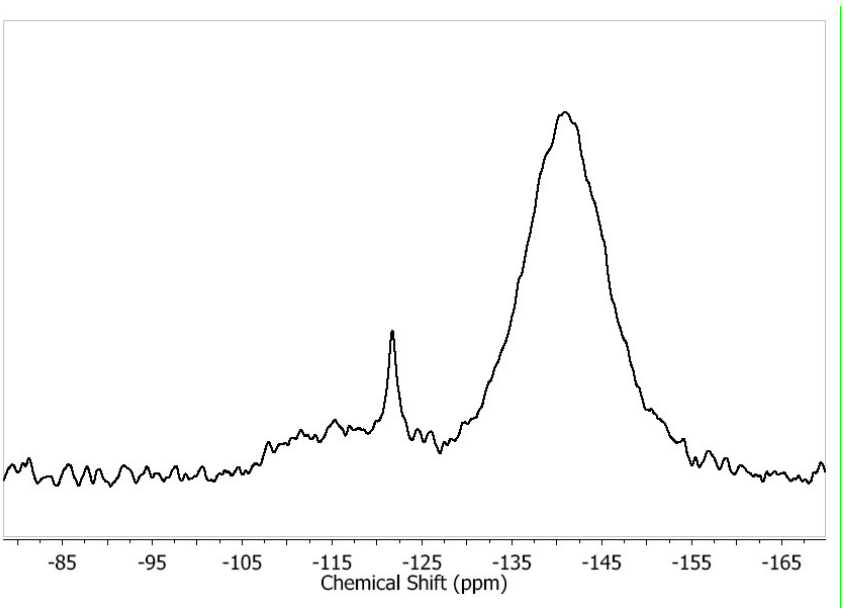

Fig. S15 Solid-state ^{19}F MAS spectrum of MM2(300) at 50 kHz. The intensity ratio of the signal at –140 ppm relative to the other smaller signals combined is 15:1.

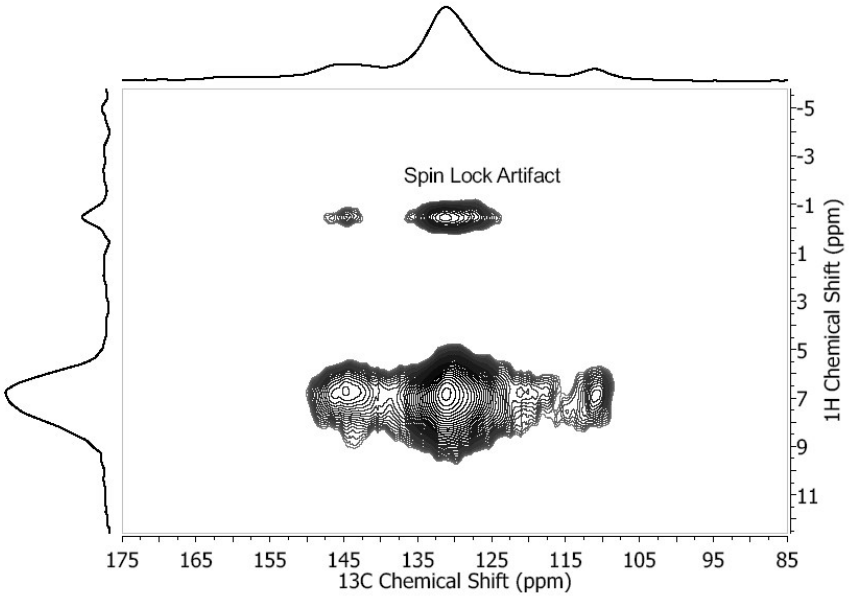

Fig. S16 $^{1}H/^{13}C$ HETCOR experiment of MM2(300) at 12 kHz spinning speed and 1.5 ms contact time.

15. References

1 A. Bhunia, V. Vasylyeva and C. Janiak, *Chem. Commun.*, 2013, **49**, 3961-3963.
2 B. Brehler, *Naturwissenschaften*, 1959, **46**, 554.
3 P. Katekomol, J. Roeser, M. Bojdys, J. Weber, and A. Thomas, *Chem. Mater.*, 2013, **25**, 542–1548
4 Y. Zhao, K. X. Yao, B. Teng, T. Zhang and Y. Han, *Energy Environ. Sci.*, 2013, **6**, 3684- 3692
5 S. Ren, M. J. Bojdys, R. Dawson, A. Laybourn, Y. Z. Khimyak, D. J. Adams and A. I. Cooper, *Adv. Mater.*, 2012, 24, 2357–2361.
6 P. Puthiaraj, S.-M. Cho, Y.-R. Lee and W.-S. Ahn, *J. Mater. Chem. A*, 2015, **3**, 6792-6797
7 H. Lim, M. C. Cha and J. Y. Chang, Macromol. *Chem. Phys.*, 2012, **13**, 1385–1390.
8 S. Xiong, X. Fu, L. Xiang, G. Yu, J. Guan, Z. Wang, Y. Du, X. Xiong and C. Pan, *Polym. Chem*., 2014, **5**, 3424-3431.
9 X. Liu, H. Li, Y. Zhang, B. Xu, S. A, H. Xia and Y. Mu, *Polym. Chem.*, 2013, **4**, 2445-2448.
10 S. Hug, M. B. Mesch, H. Oh, N. Popp, M. Hirscher, J. Senkerd and B. V. Lotsch, *J. Mater. Chem. A*, 2014, **2**, 5928-5936.
11 H. A. Patel, F. Karadas, A. Canlier, J. Park, E. Deniz, Y. Jung, M. Atilhan and C. T. Yavuz, *J. Mater. Chem.*, 2012, **22**, 8431-8437.
12 A. Bhunia, I. Boldog, A. Möller and C. Janiak, *J. Mater. Chem. A*, 2013, **1**, 14990–14999.
13 S. Nandi, U. Werner-Zwanziger and R. Vaidhyanathan, *J. Mater. Chem. A*, 2015, **3**, 21116–21122.
14 S. Dey, A. Bhunia, D. Esquivel and C. Janiak, *J. Mater. Chem. A*, 2016, **4**, 6259-6263.